Neuro-Oncology
19(10), 1408–1418, 2017 | doi:10.1093/neuonc/nox062 | Advance Access date 25 May 2017

Disrupted development and integrity of frontal white matter in patients treated for pediatric medulloblastoma

John O. Glass, Robert J. Ogg, Jung W. Hyun, Julie H. Harreld, Jane E. Schreiber, Shawna L. Palmer, Yimei Li, Amar J. Gajjar, and Wilburn E. Reddick

Departments of Diagnostic Imaging (J.O.G., R.J.O., J.H.H., W.E.R.), Biostatistics (J.W.H., Y.L.), Psychology (J.E.S., S.L.P.), and Oncology (A.J.G.), St Jude Children's Research Hospital, Memphis, Tennessee

Corresponding Author: Mr John O. Glass, Department of Diagnostic Imaging, Mail Stop 220, St. Jude Children's Research Hospital, 262 Danny Thomas Place, Memphis, TN 38105-3678 (john.glass@stjude.org).

Abstract

Background. Treatment of pediatric medulloblastoma is associated with known neurocognitive deficits that we hypothesize are caused by microstructural damage to frontal white matter (WM).

Methods. Longitudinal MRI examinations were collected from baseline (after surgery but before therapy) to 36 months in 146 patients and at 3 time points in 72 controls. Regional analyses of frontal WM volume and diffusion tensor imaging metrics were performed and verified with tract-based spatial statistics. Age-adjusted, linear mixed-effects models were used to compare patient and control images and to associate imaging changes with Woodcock–Johnson Tests of Cognitive Abilities.

Results. At baseline, WM volumes in patients were similar to those in controls; fractional anisotropy (FA) was lower bilaterally ($P < 0.001$) and was associated with decreased Processing Speed ($P = 0.014$) and Broad Attention ($P = 0.025$) performance at 36 months. During follow-up, WM volumes increased in controls but decreased in patients ($P < 0.001$) bilaterally. Smaller WM volumes in patients at 36 months were associated with concurrent decreased Working Memory ($P = 0.026$) performance.

Conclusions. Lower FA in patients with pediatric medulloblastoma compared with age-similar controls indicated that patients suffer substantial acute microstructural damage to supratentorial frontal WM following surgery but before radiation therapy or chemotherapy. Additionally, this damage to the frontal WM was associated with decreased cognitive performance in executive function 36 months later. This early damage also likely contributed to posttherapeutic failure of age-appropriate WM development and to the known association between decreased WM volumes and decreased cognitive performance.

Key words

diffusion tensor imaging | longitudinal MRI | medulloblastoma | regional analysis | tissue volumes

Medulloblastoma is the most common malignant brain tumor diagnosis in children, and following extensive therapy, their mean overall survival is 70% to 75%.[1] The standard treatment regimen of maximal surgical excision, risk-adapted craniospinal irradiation (CSI), and adjuvant chemotherapy is known to produce neurocognitive deficits in frontal lobe–mediated cognitive domains in survivors, such as working memory,[2,3] intelligence, academic performance,[4,5] processing speed,[3] and attention.[3] These deficits are known to be associated with young age at diagnosis and high-risk disease.[4] The underlying changes to the neuroanatomy that precede this quality-of-life issue are not as well known.

Previous studies successfully demonstrated that patients had a loss of white matter (WM) volume, which was greater in patients with high-risk disease who received more intensive therapy, those treated at a younger age, and those requiring intervention for hydrocephalus.[6] Furthermore,

© The Author(s) 2017. Published by Oxford University Press on behalf of the Society for Neuro-Oncology. All rights reserved.
For permissions, please e-mail: journals.permissions@oup.com

Importance of the Study

Numerous other studies of patients treated for medulloblastoma have demonstrated that survivors have reduced WM volumes often associated with known neurocognitive deficits. This finding was confirmed in this large prospective longitudinal study of 146 patients and 72 age-similar controls. Furthermore, this study was able to demonstrate that diffusion MRI measures of FA at baseline indicated that patients with medulloblastoma suffer substantial acute microstructural damage to their WM that can only be attributed to disease and/or surgical intervention. This early damage combined with the effects of radiation therapy and chemotherapy was followed by a failure of the WM volume to increase at an age-appropriate rate in patients. While decreased WM volume in survivors is known to be correlated with decreased cognitive performance, this is the first study to demonstrate decreased FA before radiation therapy or chemotherapy to be correlated with decreased cognitive performance in survivors.

decreased diffusion MRI measures of fractional anisotropy (FA), associated with decreased WM volume,[7] are most prominent in the frontal lobes[8] and mediate the impact of young age on neurocognitive performance[9] as well as other complications such as posterior fossa syndrome.[7]

The connection between the frontal lobes and the posterior fossa is being established through tract-based measures of WM integrity,[10] diaschisis,[11] and the effects of posterior fossa surgery on the distant frontal WM. A small cross-sectional study revealed that even patients with astrocytoma who undergo a posterior fossa surgical excision only demonstrate reduced frontal WM FA compared with that in healthy age-similar controls. This finding was similar, though less severe, to the impairment seen in patients with medulloblastoma.[12]

Many of the studies that have demonstrated the effects of medulloblastoma therapies have been cross-sectional in design and evaluated varying times after therapy. Longitudinal assessment of volume changes and microstructural diffusion changes would allow for more definitive evaluation of these measures as potential biomarkers of later neurocognitive impairment and further our understanding of the vulnerability of these young subjects. Additionally, early changes in the brain due to disease and surgery can be evaluated prior to additional therapies. In the current prospective study, we longitudinally examined a large cohort of pediatric patients with medulloblastoma to test the hypothesis that WM within the frontal lobes is damaged early at the microstructural level by disease and/or surgery resulting in more protracted longitudinal volumetric changes which are exacerbated by additional therapies and ultimately result in neurocognitive deficits in processing speed, attention, and working memory.

Materials and Methods

Patients and Treatment

Patients with a newly diagnosed brain tumor, between 3 and 21 years of age, were enrolled on a phase III therapeutic trial (NCT00085202) at a single institution between September 2003 and March 2013. Therapy consisted of maximal surgical resection, risk-adapted CSI, and high-dose chemotherapy for all subjects. Patients assigned to the average-risk (AR) group had minimal localized disease, while the high-risk (HR) group consisted of patients with more than 1.5 cm^2 residual disease and/or metastatic spread. The AR group received 23.4 Gy to the entire craniospinal axis, with a boost of 55.8 Gy to the primary site. The HR group received 36 Gy CSI with a boost of up to 59.4 Gy to the primary site. CSI was scheduled to begin as soon as baseline MRI evaluations were completed and would last for approximately 6 weeks. Adjuvant chemotherapy was scheduled 6 weeks after the completion of CSI, and would include 4 cycles of high-dose cyclophosphamide, cisplatin, and vincristine with stem cell support.

MRI postprocessing and analysis were completed at the following time points: baseline after surgery; after the completion of CSI (average 85 days after baseline); and 12, 18, 24, 30, and 36 months after diagnosis. MRI was a part of the clinical evaluations of these patients, and any patient unable to hold still for the examination was sedated. Treatment and imaging protocols were approved by the St Jude Institutional Review Board, and written informed consent was obtained from the patient, parent, or guardian, as appropriate.

Control Subjects

To aid in the evaluation of therapy effects, a normal healthy control population was recruited. Eligible subjects were 6–25 years old; primarily English speaking; without treatment with psychostimulants or psychotropic medications; free from major physical, neurological, or psychiatric conditions; and free from orthodontic appliances. Subjects were enrolled with a sex bias to match the patient population. They were scheduled for 3 noncontrast MRI examinations without anesthesia one year apart and screened by a board-certified neuroradiologist for incidental findings. The collection and imaging protocols were approved by the St Jude Institutional Review Board, and written informed consent was obtained from the subject, parent, or guardian, as appropriate.

Imaging Protocols

All imaging was performed on one of two 1.5T Avantos, a 3.0T Trio, or a 3.0T Skyra MRI scanner (Siemens Medical Systems). Conventional imaging consisted of whole-brain axial T1-weighted (T1w), T2-weighted

(T2w), proton density (PD), and fluid-attenuated inversion recovery (FLAIR) sequences acquired at 4- to 5-mm slice thickness with no gap and an in-plane resolution of 0.82 × 0.82 mm. T1w images were collected from a gradient echo sequence (repetition time [TR], 155–236 ms; echo time [TE], 2.52–4 ms; flip angle, 60–70 degrees), while the T2w and PD images came from a dual spin-echo sequence (TR, 4164–5310 ms; TE1, 9.4–17 ms; TE2, 94–117 ms; flip angle, 131–180 degrees). FLAIR images were acquired using a multiecho inversion recovery sequence (TR, 8030–10000 ms; TE, 103–115 ms; inversion time, 2400–2605 ms; 21 echoes).

MR diffusion tensor imaging (DTI) was acquired using bipolar diffusion-encoding gradients to reduce gradient-induced eddy currents using a double-spin echo, echo planar imaging pulse sequence (TR, 6500–10000 ms; TE, 100–120 ms, b = 700–1000 s/mm^2). Forty or more 3-mm-thick images were acquired in contiguous axial sections to provide whole-brain coverage. Using a 128-square matrix, the 192- to 230-mm field of view provided an in-plane resolution of 1.5 to 1.8 mm^2. Four acquisitions of 13 image sets were collected. The 13 image sets consisted of one in which b = 0 and 12 noncollinear, noncoplanar diffusion-gradient directions in which b = 700 to 1000 s/mm^2 to calculate the diffusion tensor for each voxel. This acquisition is a compromise to ensure the highest signal-to-noise ratio possible within a limited amount of time to minimize the risk/benefit ratio for this population.

Image Analysis

For volumetric WM analysis, the T2w images from all examinations of each subject were first registered together using the rigid-body registration tools provided in the VTK CISG Registration Toolkit 2.0.[13] The remaining conventional image sets were then aligned to the T2w image in the subject's space using the same tools. Brain parenchyma masks were then computed before performing inhomogeneity correction.[14] Finally, WM, gray matter, and cerebrospinal fluid volumes were segmented using a Kohonen self-organizing network technique based on T1w, T2w, PD, and FLAIR images.[15,16] Repeated measures of WM and gray matter demonstrate a predicted variance of approximately 2% with these methods.[16]

Voxel-wise tensor calculations were performed in SPM8 (http://www.fil.ion.ucl.ac.uk/spm/) by using the DTI toolkit. Each of the 4 acquisitions was aligned to remove eddy-current drift and patient motion before being averaged together. Tensor deconvolution was used to calculate tensors and derive the eigenvectors and eigenvalues. Eigenvalues were combined into the following parametric maps: FA, radial (RAD), and axial (AX) diffusivity. AX is the largest eigenvalue in the direction of the WM tract, while RAD consists of the 2 remaining eigenvalues perpendicular to the tract. Output maps were registered to the segmentation data by performing a rigid-body alignment of the first b = 0 image, the reference for all tensor calculations, and the registered T2w image for each examination.

Regional Analysis

Seven anatomical slices at the level of the basal ganglia, including the genu and splenium of the corpus callosum, the putamen, and lateral ventricles, were selected for our representative volumetric studies.[17–19] To further examine the localization of systematic treatment effects, these 7 slices were divided into quadrants by using a modification of the technique reported previously.[20] Briefly, the plane between the most anterior midpoint of the genu and the most posterior midpoint of the splenium forms a division between the left and right hemispheres. A perpendicular plane at the midpoint of the 2 selected points divides the anterior and posterior sections of the brain. We then limited our study to the left and right anterior quadrants, because those regions are hypothesized to support executive function and attention and have been demonstrated previously to be more susceptible to damage during therapy.[8,20] Each region was evaluated for changes in WM volume, FA, RAD, and AX within the segmented normal-appearing WM volume.

Tract-Based Spatial Statistics

In addition to the regional analysis, FA maps were processed via the Tract-Based Spatial Statistics (TBSS) pipeline, part of the FMRIB Software Library (FSL, http://www.fmrib.ox.ac.uk/fsl), which minimizes intersubject variability and is therefore more reliable than other techniques.[21] TBSS depends on the registration of all FA maps to a common atlas space. This was completed using the nonlinear registration tools in FSL, and the FA images were normalized from each subject to the FMRIB58_FA standard space in the Montreal Neurologic Institute coordinates. After registration, the mean image of all subjects was calculated to identify all WM voxels by using an FA lower threshold of 0.25. The mean WM was then skeletonized, and the final WM skeleton represented the fiber bundle centers across patients and control subjects. The FA data from each subject was then mapped onto the skeleton to represent the true physiological difference for each subject, without bias to the alignment or structural variability of the subjects. After statistical analysis, the identified regions were labeled anatomically using the JHU-ICBM-DTI-81 WM atlas.[22] Fiber tracts were grouped according to anatomical and functional associations with larger fiber bundles.[23]

Neuropsychological Data

To assess the impact of the observed changes in WM, neuropsychological scores were correlated to the imaging metrics. Neurocognitive assessments were scheduled at baseline and yearly afterward using the Woodcock–Johnson Tests of Cognitive Abilities Third Edition[24] to evaluate Processing Speed, Working Memory, Broad Attention, and General Intellectual Ability. These age-adjusted standardized scores were used in the analyses and had a population mean of 100 and a standard deviation of 15. Only subjects with both imaging at baseline and/or 36 months and neurocognitive assessments at 36 months were

included in this ad-hoc analysis. The full neuropsychological assessment for this population has been reported previously.[3,4]

Statistical Analysis

To analyze the repeated measures in the longitudinal data, linear mixed-effects modeling was performed using the restricted maximum likelihood estimation method. Separate models were computed for each regional output measure, as well as for each pixel in the TBSS analysis, and multiple comparisons were corrected using the false discovery rate (FDR).[25] Covariates of our first 2-group models (Eq. 1) included time after radiation therapy (in months), age at baseline (in years), and subject group (control or patient). After establishing that some differences existed between patients and controls, we implemented a 3-group model (Eq. 2) and divided the patient group into an AR group and an HR group, based on disease risk stratification. These 2 sets of models, with intercepts and slopes that varied randomly among individuals, are represented by the following equations:

$$Y_{ij} = \beta_0 + \beta_1 t_{ij} + \beta_2 BaseAge_i + \beta_3 Patient + \beta_4 t_{ij} \times Patient + b_{0i} + b_{1i} t_{ij} + \varepsilon_{ij} \quad (1)$$

$$Y_{ij} = \beta_0 + \beta_1 t_{ij} + \beta_2 BaseAge_i + \beta_3 AR_i + \beta_4 HR_i + \beta_5 t_{ij} \times AR_i + \beta_6 t_{ij} \times HR_i + b_{0i} + b_{1i} t_{ij} + \varepsilon_{ij}, \quad (2)$$

where Y_{ij} is the parameter score for the ith subject at the jth observation; β is the parameter fit by the model; t represents time after radiation therapy; *BaseAge* is the age of the subject at baseline; and *Patient, HR,* or *AR* represents the appropriate patient group (variable set to 1 when appropriate and set to 0 otherwise). The inclusion of age at baseline served to control all imaging metrics for differences attributable to age. To test the difference in the change of the response between the groups, both models included an interaction term between time and group. The model produced a slope and intercept for the controls and then terms to adjust the patient grouping from the controls. By combining these 2 terms, we produced estimates for the baseline value of each parameter (intercept) and the change in the parameter over the 36-month study (slope).

Model estimates were further analyzed to evaluate the effects of various covariates on the parameter scores. A likelihood-ratio test was used to assess the differences in baseline value and change over time between groups (control and patient) or across all 3 groups (control, AR, and HR). A significant result indicated that the change over time or baseline value was not the same across groups. When the likelihood-ratio test rejected the null hypothesis that the change over time or baseline value was the same across all 3 groups, a Wald test was done to determine whether there were significant differences between the risk arms (AR vs HR). A significant result indicated that the change over time or baseline value for the 2 patient groups was statistically different.

The final analysis used multiple linear regression models with individual neurocognitive measures at 36 months as a response variable and the imaging parameter, age, and risk arm as covariates. The model can be expressed as

$$Y_i = \beta_0 + \beta_1 \mathrm{Img}_i + \beta_2 Age_i + \beta_3 Group + \varepsilon_i. \quad (3)$$

To test the association of the neurocognitive performance measures with the imaging parameter, we used a *t*-test. All analyses were corrected for multiple comparisons with the FDR procedure.

Results

Subject Characteristics

There were a total of 207 subjects enrolled on this prospective clinical trial at the primary institution. Of those 207 subjects, 61 were excluded from this study for the following reasons: primary tumor type not medulloblastoma (n = 52), surgical resection or active tumor inside the volume of interest (n = 2), and no evaluable MRI examinations (n = 7). The 146 subjects who participated in this study consisted of 96 male patients and 50 female patients. The median age at diagnosis was 8.7 years (range, 3.2–21.6 y); 93 subjects had AR disease, and 53 had HR disease. There were a total of 72 control subjects who completed all 3 time points. These subjects consisted of 44 male subjects and 28 female subjects. Their median age at study enrollment was 13.0 years (range, 6.0–24.5 y).

Imaging Examinations

A total of 864 evaluable MRI examinations were completed (502 required sedation) for the 146 patients studied (Table 1). Eleven examinations were not completed at the appropriate time point and thus were considered missing data. Sixteen examinations were not evaluable due to metal artifacts that prevented analysis. One 18-month examination demonstrated an epidural hematoma in the volume of interest that resolved before the next examination, and the single time point was excluded from analysis. Thirty-two patients went off protocol or were no longer followed at later time points for the following reasons: progressive disease (n = 15), patient death (n = 13), stroke in the volume of interest (n = 2), renal complications that prevented contrast administration (n = 1), and development of a second malignancy (n = 1) (Table 1). Normalization was unsuccessful in 12 examinations primarily due to ventriculomegaly. These examinations were excluded from the TBSS analysis but were included in the regional analyses. Twenty-one DTI datasets were missing for the following reasons: metal artifact that prevented normalization (n = 7), acquisition placement (n = 1), missed acquisition (n = 11), and technical failures (n = 2). These 21 examinations were included in the regional analysis without DTI measures but were excluded from the TBSS analysis.

A total of 215 evaluable MRI examinations were acquired in the 72 control subjects studied (Table 1). One baseline examination was excluded from both regional and TBSS analyses due to subject motion. Additionally, one baseline examination did not have conventional sequences for regional analysis, but the DTI was usable for TBSS analysis.

Table 1 Number of MRI examinations and types of data analysis done at each time point

Group	Analysis	Number of MRI Examinations[a]						
		Baseline	Post-RT	12 mo	18 mo	24 mo	30 mo	36 mo
Patients	Regional	142	144	128	116	114	112	108
	TBSS	124	141	128	114	111	108	105
	Off-protocol[b]	0	0	14	25	28	31	32
Controls	Regional	70		72		72		
	TBSS	71		72		72		

Abbreviation: RT, radiation therapy.
[a]The data represent the number of patients imaged at each time point.
[b]Off-protocol indicates the number of patients who were lost to analysis.

Regional Analysis

When the frontal WM volume was compared between patients and controls, there was no difference between the 2 groups at baseline (Table 2). However, there was a significant difference in the frontal WM volume change over time, with an increase in WM volume for the controls and a decrease in the patients. There were no differences in frontal WM volume between control, HR, and AR subjects at baseline (Table 3). However, the change in frontal WM volume over time significantly differed across all 3 groups. The control group showed an increase in WM volume over time, the AR group had a flat or very small decrease in WM volume over time, and the HR group showed a distinct decrease (Fig. 1A). While the HR group had a greater decline than the AR group, this difference did not reach statistical significance.

Analysis of DTI metrics revealed that patients had significantly lower bilateral FA and AX at baseline than did controls (Table 2). RAD measurements showed higher diffusivity at baseline in patients but only reached significance in the right frontal lobe. Changes in FA, AX, and RAD over time differed significantly between the patients and controls (Fig. 1B–D). Controls had very little change in FA over time, while patients showed an increase with time. AX and RAD showed no change over time for the controls, but both distinctly decreased in patients. Compared with the AR group, the HR group demonstrated a significantly lower baseline FA bilaterally, but AX and RAD at baseline were not statistically different for these 2 groups. The change in FA, AX, and RAD over time was not statistically different for the AR and HR groups (Table 3).

TBSS Analysis

Results of the regional analysis were further assessed using a TBSS analysis to evaluate where the results could be confirmed globally. The skeleton calculated for the 1089 MRI examinations included in this study contained 89 456 voxels covering the entire brain. TBSS analysis of FA showed that 84 895 (95%) voxels confirmed that baseline FA was significantly lower in patients than in controls, even after adjusting for age. When examining the change in FA over time, 10 753 (12%) voxels demonstrated a significant difference between patients and controls. Limiting the longitudinal analysis to only those voxels with a significantly decreased FA at baseline revealed that patients had increased FA over time in 8117 (76%) voxels and decreased FA over time in 2199 (21%) voxels. The first group of voxels matches the pattern seen in the regional analysis, while the latter group suggests additional damage occurs over time in some regions illustrated in Fig. 2. When we compared the AR and HR groups, we found no significant voxel-based differences for either the baseline FA or the change in FA over time.

For voxels with increasing FA over time, in patients versus controls, 4020 of 8117 (50%) were located within the JHU-ICBM-DTI-81 WM atlas.[22] The primary tracts identified by this atlas were the corona radiata and the corpus callosum (Table 4). For voxels where FA in patients was decreasing over time compared with the controls, 939 of 2199 (43%) were located within the atlas. Primary tracts identified in the patients with decreasing FA included the cerebellar peduncle, cingulum, internal capsule, and corticospinal tract (Table 4).

Neuropsychological Data

Ninety-two patients had both complete imaging at baseline and/or 36 months and neurocognitive assessments at 36 months. Performance was considered to be impaired if the individual score was more than one standard deviation below the normative mean, which should include approximately 16% of subjects. One of the lowest average composite scores investigated was Processing Speed (84.0 ± 21.0; mean ± standard deviation) with 44.3% of subjects being impaired. Next, we considered Broad Attention (89.6 ± 18.0; mean ± standard deviation), which was impaired in 36.5% of subjects. The 2 remaining composite measures, Working Memory (94.4 ± 16.4; mean ± standard deviation) and General Intellectual Ability (95.6 ± 18.2; mean ± standard deviation) were much closer to the normative distribution with only 25.6% and 27.8%, respectively, impaired.

Table 2 Changes in white matter volume and DTI metrics in the frontal regions of patients with pediatric medulloblastoma tumors and healthy controls

Regional Metric	Left Anterior Frontal Region				Right Anterior Frontal Region			
	Baseline		Change over Time		Baseline		Change over Time	
	P-value[a]	Dir[b]	*P*-value[a]	Dir[b]	*P*-value[a]	Dir[b]	*P*-value[a]	Dir[b]
WMv	ns	—	<0.001	P < C	ns	—	<0.001	P < C
FA	<0.001	P < C	<0.001	P > C	<0.001	P < C	0.004	P > C
AX	<0.001	P < C	0.001	P < C	<0.001	P < C	0.001	P < C
RAD	ns	—	<0.001	P < C	0.026	P > C	<0.001	P < C

Abbreviations: AX, axial diffusivity; C, control group; Dir, direction; DTI, diffusion tensor imaging; FA, fractional anisotropy; ns, not significant; P, patient group; RAD, radial diffusivity, WMv, white matter volume.
[a]The likelihood ratio test was used to compare the groups, and $P < 0.05$ was considered statistically significant.
[b]Direction indicates which group (patients vs controls) had the higher value for that specific metric.

Table 3 Comparison of changes in white matter volume and DTI metrics of patients with average- or high-risk pediatric medulloblastoma tumors and those in healthy controls

Regional Metric	Baseline				Change over Time			
	All Groups		AR vs. HR		All Groups		AR vs. HR	
	P-value[a]	Dir[b]	P-value[a]	Dir[b]	*P*-value[a]	Dir[b]	*P*-value[a]	Dir[b]
antL								
WMv	ns	—	—	—	<0.001	P < C	ns	—
FA	<0.001	P < C	0.041	HR < AR	0.001	P > C	ns	—
AX	<0.001	P < C	ns	—	0.003	P < C	ns	—
RAD	ns	—	—	—	<0.001	P < C	ns	—
antR								
WMv	ns	—	—	—	<0.001	P < C	ns	—
FA	<0.001	P < C	0.038	HR < AR	0.017	P > C	ns	—
AX	<0.001	P < C	ns	—	0.002	P < C	ns	—
RAD	0.019	P > C	ns	—	<0.001	P < C	ns	—

Abbreviations: antL, left anterior frontal region; antR, right anterior frontal region; AR, average-risk group; AX, axial diffusivity; C, control group; Dir, direction; DTI, diffusion tensor imaging; FA, fractional anisotropy; HR, high-risk group; ns, not significant; P, patient group; RAD, radial diffusivity, WMv, white matter volume.
[a]The likelihood ratio test was used to compare all 3 groups, and the Wald test was used to compare the average-risk vs high-risk groups. $P < 0.05$ was considered a statistically significant change.
[b]Direction indicates which group had the higher value for that specific metric.

At 36 months, WM volume, which had diverged over time in patients compared with the controls, was positively associated with Working Memory performance ($P = 0.026$). Smaller frontal lobe WM volumes in patients were significantly associated with lower Working Memory performance after adjusting for age. Baseline FA measures were significantly lower in patients than controls and were significantly associated with Processing Speed ($P = 0.014$) and Broad Attention ($P = 0.025$) measures at 36 months. FA also demonstrated a trending association with Working Memory ($P = 0.062$) and General Intellectual Ability ($P = 0.062$). All associations were positive such that lower frontal lobe FA corresponded to decreased neurocognitive performance 36 months later even after adjusting for age.

Discussion

The results of this study characterize the time course of microstructural and global changes in the frontal WM associated with disease, surgery, radiation therapy, and adjuvant chemotherapy in 146 children treated for medulloblastoma (864 MRI examinations) and 72 age-similar healthy controls (215 MRI examinations). Results from this large longitudinal study supported previous work showing that WM volume was decreased in a similar cohort at the end of follow-up.[6] Additionally, our results confirmed that WM volumes of controls and patients were comparable at the baseline evaluation, but subsequently decreased over time in patients. The smaller frontal WM volumes in

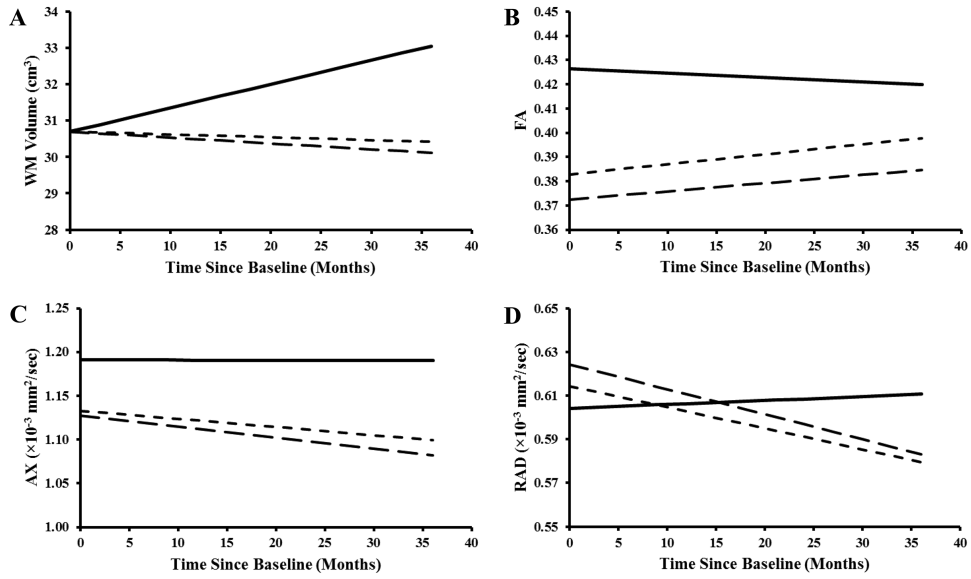

Fig. 1 Modeled trajectories of (A) white matter volume, (B) fractional anisotropy, (C) axial diffusivity, and (D) radial diffusivity in the right frontal regions of the 3 study groups: controls (solid lines), patients with average-risk disease (dotted lines), and those with high-risk disease (dashed lines). The baseline age assumed for this demonstrative purpose is 8 years for all 4 graphs.

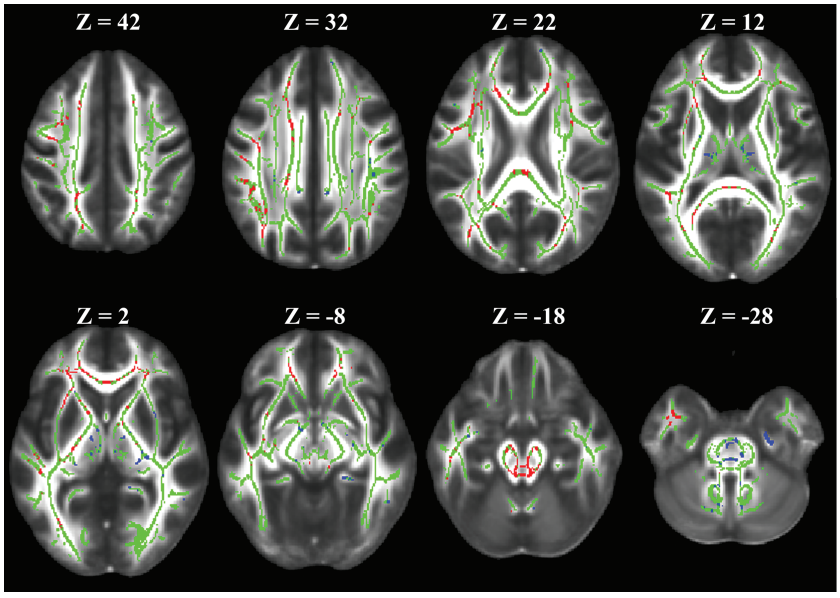

Fig. 2 Representative images of the TBSS analysis. The images shown are on top of the FMRIB58_FA standard space. The skeleton voxels are presented in green. Voxels where the change in FA over time is greater in patients than in controls are shown in red and confirm the regional analysis results. Voxels where the change in FA over time is lower in patients than in controls are shown in blue and represent specific locations that are not recovering after therapy. The Z position is given in Montreal Neurologic Institute Atlas dimension as a reference.

patients were significantly associated with decreased Working Memory performance. Baseline FA was lower in patients and then increased at a faster rate than in controls but never reached age-appropriate levels. The TBSS analysis enabled us to discern the spatial localization of voxels with this pattern of FA within the brain, predominantly in

Table 4 TBSS analysis of white matter tracts in patients with pediatric medulloblastoma tumors and healthy controls

Brain Region	Patients > Controls[a]		Patients < Controls[b]	
	Pixel Count	% in Atlas[c]	Pixel Count	% in Atlas[c]
Corpus callosum	919	22.9	40	4.3
Corticospinal tract	19	0.5	109	11.6
Medial lemniscus	29	0.7	10	1.1
Cerebellar peduncle	284	7.1	296	31.5
Cerebral peduncle	220	5.5	15	1.6
Internal capsule	374	9.3	133	14.2
Corona radiata	1455	36.2	62	6.6
Posterior thalamic radiation	203	5.0	1	0.1
Sagittal stratum	19	0.5	15	1.6
External capsule	268	6.7	45	4.8
Cingulum	13	0.3	167	17.8
Fornix	15	0.4	14	1.5
Superior longitudinal fasciculus	181	4.5	31	3.3
Superior fronto-occipital fasciculus	12	0.3	0	0.0
Uncinate fasciculus	8	0.2	1	0.1
Tapetum	1	0.0	0	0.0

[a]Voxels where the change in FA over time is greater in patients than in controls represent recovery of the damaged white matter tracts and bundles.
[b]Voxels where the change in FA over time is smaller in patients than in controls represent damaged white matter tracts and bundles that are not recovering from damage.
[c]The *JHU-ICBM-DTI-81 WM Atlas*[23] provides information about the major white matter tracts and bundles, but it is not inclusive of all the regions analyzed by the TBSS pipeline.

the corpus callosum and corona radiata. Smaller regions in the cerebellar peduncle and internal capsule demonstrated a pattern of reduced baseline FA, which further decreased over time. This result may identify a particularly vulnerable set of WM tracts, but further study would be needed.

These results highlight the impact of disease and surgical removal of posterior fossa tumors on the structure of the distant supratentorial brain. WM volume of patients decreased throughout therapy and during follow-up. This finding is consistent with the WM volume being a marker of global damage that occurs after the accumulation of microstructural or cellular damage. When we examined the DTI metrics at baseline, after surgery but before any therapy, we found evidence of preexisting microstructural damage; the FA was significantly lower in the patients than in the controls. Furthermore, this early microstructural damage was significantly associated with decreased neurocognitive function at 36 months.

Reukriegel et al reported reduced FA in the supratentorial brains of patients with pilocytic astrocytoma approximately 2 years after surgery and in patients with medulloblastoma approximately 4 years after surgery, radiation therapy, and chemotherapy.[12] Law et al reported that patients with low-grade posterior fossa glioma treated with surgical excision alone demonstrated reduced FA and higher RAD than controls in the cerebello-thalamo-cerebral pathway.[26] Our data support these previous findings and suggest that significant damage occurs to the immature brain as a result of disease and/or surgical excision, as changes are seen before any additional therapy is administered. Given the location of the primary medulloblastoma lesions, damage to the dentate nuclei or the associated efferent cerebellar pathway by growth of the lesion over time and the addition of surgical resection may have more global repercussions for frontal supratentorial white matter.[10,11,27] Although surgical intervention will remain paramount to successfully cure medulloblastoma, the adverse effect of tumor and surgery distally to the surgical site, in the supratentorial brain, must be noted.

All modeling of differences between the patient and control groups depended on the normal developmental patterns demonstrated by the controls. As expected, WM volume in control subjects increased over time, and the baseline volume was higher with older age. DTI metrics also demonstrated expected developmental trajectories in controls: baseline FA was higher, and baseline AX and RAD were lower with older age.[28] Although our control subjects demonstrated small age-appropriate changes in their DTI metrics over the 2 years that they were followed, the changes did not reach statistical significance, perhaps because WM DTI measures in control subjects, who were an average of 13 years of age at study enrollment, may have been asymptotically approaching adult values and would be expected to change very little over this relatively short study period. Any difference in age between patients and controls was accounted for by including age at baseline in the linear mixed effects models. Changes in the patient group, however, were large enough to be readily

appreciable and confirmed by TBSS analysis. The regional analysis detected a significant difference in baseline FAs across the 3 groups (controls > AR > HR), but the TBSS analysis, which fit the model at each voxel in the skeleton, did not detect this difference. This discrepancy was most likely due to the decreased sensitivity with lower signal-to-noise ratios in a single voxel compared with that in an averaged volume.

Our results suggest the presence of acute, early microstructural WM damage by disease and/or surgical intervention. Baseline FA was decreased in patients, similar to changes seen in acute ischemia,[29] but the accompanying increase in RAD is not typical of ischemia and there was no imaging evidence of infarction, suggesting an alternative mechanism. Baseline AX was decreased, which may occur due to the accumulation of cellular debris, disordering of microtubule arrangement, and filament aggregation in acute axonal injury.[30] Additional axonal injury during therapy, reflected in the longitudinal decreases in RAD and AX, may be due to regional cell infiltration and cellular swelling, reduced extracellular fluid volume, and overall restricted diffusion.[30–32] Animal models have shown that acute injury involving axonal swelling with minimal axonal damage may be reflected in decreased AX.[30]

Because the rate of decrease in RAD was greater than that in AX, the FA increased. Furthermore, the subsequent near-normalizing increase in FA over the 3-year course of treatment and follow-up combined with macroscopic WM volume loss suggests overall loss of cellular density despite evidence of microstructural recovery, potentially due to loss of support cells (glia), axons, and/or myelin, without which DTI parameters may be near-normal if axonal density is maintained.[33]

As with any study, the limitations must be taken into account when interpreting the results. While an ideal imaging study would use a single MR scanner, this longitudinal study that spanned 13 years could not be limited to only one scanner. Imaging quality was constantly monitored to ensure consistent results across all scans. Two different field strengths were used to acquire the MR imaging in this study. However, since the primary results reported for this study were longitudinal, imaging within an individual subject was acquired at the same field strength. DTI metrics of FA and diffusivity are dependent on the underlying architecture of the microstructure within the voxel and is not anticipated to be significantly affected by field strength. However, the signal-to-noise ratio of the measurements is influenced by field strength and has a significant impact on the uncertainty of the calculated metrics.[34] This could theoretically produce a slight overestimation of the FA metric at lower signal-to-noise ratio, but this should be negligible for b-values used in typical clinical imaging.[34] While one early study found significantly higher FA values at 3.0T compared with 1.5T,[35] the preponderance of the published evidence supports the assumption of negligible differences in measures of FA and diffusivity as a function of MR field strength.[36–39]

Although this study was longitudinal in design, the control subjects were followed for only 2 years, while the patients were followed for 3 years. At the same time, 32 of 146 (22%) patients were no longer followed at the 3-year time point due to therapy failure, death, treatment complications, or the development of a second malignancy. This could limit the model's accuracy at the later time points. Our initial imaging assessment was after surgical resection but before the beginning of therapy. This limitation was driven by the unique referral pattern at our institution, where patients usually receive initial resection of their primary tumor before referral. Therefore, the study was unable to distinguish between effects of disease and surgery. While controls were never sedated, a large proportion of the patient examinations involved sedation. Sedation is known to affect cerebral perfusion but there is no evidence of differences between DTI with or without sedation. This study was designed as a prospective trial of 2 risk-adapted therapeutic regimens and was not designed to weigh the differences between varying other treatment methods. Another limitation of our study was the regional measures, which were performed over a limited volume and only in the frontal regions. This longitudinal clinical study was designed more than 14 years ago and represented the state-of-the-art imaging research at that time. However, recognizing this limitation, we performed the TBSS analysis across the whole brain, which confirmed the findings of the more limited regional analyses and facilitated the parcellation of the significant voxels into WM fiber tracts based on the probabilistic tract atlas.

In conclusion, DTI metrics indicate that patients with pediatric medulloblastoma suffer substantial acute microstructural damage to supratentorial WM even before radiation therapy or chemotherapy, attributable only to disease and/or surgical intervention and associated with decreased cognitive performance in survivors 36 months later. This early damage may contribute to posttherapeutic failure of age-appropriate WM development and to the known association between decreased WM volumes and decreased cognitive performance in survivors of childhood medulloblastoma.

Funding

This work was supported in part by Cancer Center Support Grant P30 CA-21765 from the National Cancer Institute, grant HD049888 from the National Institute of Child Health and Human Development, grant RR029005 from the National Center for Research Resources, and ALSAC.

Acknowledgments

We acknowledge the valuable contributions of Rhonda Simmons, advanced signal processing technician. We also gratefully thank Angela McArthur for editorial assistance.

Conflict of interest statement. The authors declare no conflicts of interest.

References

1. Gajjar AJ, Robinson GW. Medulloblastoma-translating discoveries from the bench to the bedside. *Nat Rev Clin Oncol*. 2014;11(12):714–722.
2. Knight SJ, Conklin HM, Palmer SL, et al. Working memory abilities among children treated for medulloblastoma: parent report and child performance. *J Pediatr Psychol*. 2014;39(5):501–511.
3. Palmer SL, Armstrong C, Onar-Thomas A, et al. Processing speed, attention, and working memory after treatment for medulloblastoma: an international, prospective, and longitudinal study. *J Clin Oncol*. 2013;31(28):3494–3500.
4. Schreiber JE, Gurney JG, Palmer SL, et al. Examination of risk factors for intellectual and academic outcomes following treatment for pediatric medulloblastoma. *Neuro Oncol*. 2014;16(8):1129–1136.
5. Moxon-Emre I, Bouffet E, Taylor MD, et al. Impact of craniospinal dose, boost volume, and neurologic complications on intellectual outcome in patients with medulloblastoma. *J Clin Oncol*. 2014;32(17):1760–1768.
6. Reddick WE, Glass JO, Palmer SL, et al. Atypical white matter volume development in children following craniospinal irradiation. *Neuro Oncol*. 2005;7(1):12–19.
7. Soelva V, Hernáiz Driever P, Abbushi A, et al. Fronto-cerebellar fiber tractography in pediatric patients following posterior fossa tumor surgery. *Childs Nerv Syst*. 2013;29(4):597–607.
8. Qiu D, Kwong DL, Chan GC, Leung LH, Khong PL. Diffusion tensor magnetic resonance imaging finding of discrepant fractional anisotropy between the frontal and parietal lobes after whole-brain irradiation in childhood medulloblastoma survivors: reflection of regional white matter radiosensitivity? *Int J Radiat Oncol Biol Phys*. 2007;69(3):846–851.
9. Palmer SL, Glass JO, Li Y, et al. White matter integrity is associated with cognitive processing in patients treated for a posterior fossa brain tumor. *Neuro Oncol*. 2012;14(9):1185–1193.
10. Law N, Greenberg M, Bouffet E, et al. Visualization and segmentation of reciprocal cerebrocerebellar pathways in the healthy and injured brain. *Hum Brain Mapp*. 2015;36(7):2615–2628.
11. Miller NG, Reddick WE, Kocak M, et al. Cerebellocerebral diaschisis is the likely mechanism of postsurgical posterior fossa syndrome in pediatric patients with midline cerebellar tumors. *AJNR Am J Neuroradiol*. 2010;31(2):288–294.
12. Rueckriegel SM, Driever PH, Blankenburg F, Lüdemann L, Henze G, Bruhn H. Differences in supratentorial damage of white matter in pediatric survivors of posterior fossa tumors with and without adjuvant treatment as detected by magnetic resonance diffusion tensor imaging. *Int J Radiat Oncol Biol Phys*. 2010;76(3):859–866.
13. Rueckert D, Frangi AF, Schnabel JA. Automatic construction of 3-D statistical deformation models of the brain using nonrigid registration. *IEEE Trans Med Imaging*. 2003;22(8):1014–1025.
14. Ji Q, Glass JO, Reddick WE. A novel, fast entropy-minimization algorithm for bias field correction in MR images. *Magn Reson Imaging*. 2007;25(2):259–264.
15. Glass JO, Reddick WE, Reeves C, Pui CH. Improving the segmentation of therapy-induced leukoencephalopathy in children with acute lymphoblastic leukemia using a priori information and a gradient magnitude threshold. *Magn Reson Med*. 2004;52(6):1336–1341.
16. Reddick WE, Glass JO, Cook EN, Elkin TD, Deaton RJ. Automated segmentation and classification of multispectral magnetic resonance images of brain using artificial neural networks. *IEEE Trans Med Imaging*. 1997;16(6):911–918.
17. Blatter DD, Bigler ED, Gale SD, et al. Quantitative volumetric analysis of brain MR: normative database spanning 5 decades of life. *AJNR Am J Neuroradiol*. 1995;16(2):241–251.
18. Glass JO, Ji Q, Glas LS, Reddick WE. Prediction of total cerebral tissue volumes in normal appearing brain from sub-sampled segmentation volumes. *Magn Reson Imaging*. 2003;21(9):977–982.
19. Matsumae M, Kikinis R, Mórocz IA, et al. Age-related changes in intracranial compartment volumes in normal adults assessed by magnetic resonance imaging. *J Neurosurg*. 1996;84(6):982–991.
20. Reiss AL, Abrams MT, Singer HS, Ross JL, Denckla MB. Brain development, gender and IQ in children. A volumetric imaging study. *Brain*. 1996;119 (Pt 5):1763–1774.
21. Smith SM, Jenkinson M, Johansen-Berg H, et al. Tract-based spatial statistics: voxelwise analysis of multi-subject diffusion data. *Neuroimage*. 2006;31(4):1487–1505.
22. Mori S, Oishi K, Jiang H, et al. Stereotaxic white matter atlas based on diffusion tensor imaging in an ICBM template. *Neuroimage*. 2008;40(2):570–582.
23. Yu HJ, Christodoulou C, Bhise V, et al. Multiple white matter tract abnormalities underlie cognitive impairment in RRMS. *Neuroimage*. 2012;59(4):3713–3722.
24. Woodcock R, McGraw K, Mather N. *Woodcock-Johnson Third Edition, Tests of Cognitive Abilities*. Itasca, IL: Riverside Publishing; 2001.
25. Benjamini Y, Hochberg Y. Controlling the false discovery rate—a practical and powerful approach to multiple testing. *J Roy Stat Soc B Met*. 1995;57(1):289–300.
26. Law N, Bouffet E, Laughlin S, et al. Cerebello-thalamo-cerebral connections in pediatric brain tumor patients: impact on working memory. *Neuroimage*. 2011;56(4):2238–2248.
27. Law N, Smith ML, Greenberg M, et al. Executive function in paediatric medulloblastoma: The role of cerebrocerebellar connections. *J Neuropsychol*. 2015;doi: 10.1111/jnp.12082.
28. Simmonds DJ, Hallquist MN, Asato M, Luna B. Developmental stages and sex differences of white matter and behavioral development through adolescence: a longitudinal diffusion tensor imaging (DTI) study. *Neuroimage*. 2014;92:356–368.
29. Tuor UI, Morgunov M, Sule M, et al. Cellular correlates of longitudinal diffusion tensor imaging of axonal degeneration following hypoxic-ischemic cerebral infarction in neonatal rats. *Neuroimage Clin*. 2014;6:32–42.
30. Aung WY, Mar S, Benzinger TL. Diffusion tensor MRI as a biomarker in axonal and myelin damage. *Imaging Med*. 2013;5(5):427–440.
31. Arfanakis K, Haughton VM, Carew JD, Rogers BP, Dempsey RJ, Meyerand ME. Diffusion tensor MR imaging in diffuse axonal injury. *AJNR Am J Neuroradiol*. 2002;23(5):794–802.
32. Stidworthy MF, Genoud S, Suter U, Mantei N, Franklin RJ. Quantifying the early stages of remyelination following cuprizone-induced demyelination. *Brain Pathol*. 2003;13(3):329–339.
33. van der Voorn JP, Pouwels PJ, Hart AA, et al. Childhood white matter disorders: quantitative MR imaging and spectroscopy. *Radiology*. 2006;241(2):510–517.
34. Jones DK, Basser PJ. "Squashing peanuts and smashing pumpkins": how noise distorts diffusion-weighted MR data. *Magn Reson Med*. 2004;52(5):979–993.
35. Huisman TA, Loenneker T, Barta G, et al. Quantitative diffusion tensor MR imaging of the brain: field strength related variance of apparent diffusion coefficient (ADC) and fractional anisotropy (FA) scalars. *Eur Radiol*. 2006;16(8):1651–1658.

36. Choi S, Cunningham DT, Aguila F, et al. DTI at 7 and 3 T: systematic comparison of SNR and its influence on quantitative metrics. *Magn Reson Imaging*. 2011;29(6):739–751.

37. Hunsche S, Moseley ME, Stoeter P, Hedehus M. Diffusion-tensor MR imaging at 1.5 and 3.0 T: initial observations. *Radiology*. 2001;221(2):550–556.

38. Notohamiprodjo M, Dietrich O, Horger W, et al. Diffusion tensor imaging (DTI) of the kidney at 3 tesla-feasibility, protocol evaluation and comparison to 1.5 Tesla. *Invest Radiol*. 2010;45(5):245–254.

39. Polders DL, Leemans A, Hendrikse J, Donahue MJ, Luijten PR, Hoogduin JM. Signal to noise ratio and uncertainty in diffusion tensor imaging at 1.5, 3.0, and 7.0 Tesla. *J Magn Reson Imaging*. 2011;33(6):1456–1463.